Supplementary Information

Cu-modulated PtCr Intermetallic Nanoparticles: Balancing Activity and Durability for Efficient Oxygen Reduction Reaction

Gongao Peng [ab], Chengyu Li [a], Peng Qin [ab], Jiaqi Zhao [a], Lu Shang *[ac] and Tierui Zhang *[ab]

a Key Laboratory of Photochemical Conversion and Optoelectronic Materials, Technical Institute of Physics and Chemistry, Chinese Academy of Sciences, Beijing 100190, China.
b Center of Materials Science and Optoelectronics Engineering, University of Chinese Academy of Sciences, Beijing 100049, China.
c School of Chemistry and Chemical Engineering, Nanjing University of Science and Technology, Nanjing 210094, China.
*Correspondence and requests for materials should be addressed to Lu Shang (shanglu@njust.edu.cn) or Tierui Zhang (tierui@mail.ipc.ac.cn)

Contents

Experimental Section

Chemicals and materials

Tetrapropoxysilane (TPOS, 97 wt.%), tetraethoxysilane (TEOS, 99 wt.%), resorcinol (99 wt.%), platinum (II) acetylacetonate ($Pt(acac)_2$, 98 wt.%) and ethanol (99.9 wt.%) were purchased from Innochem. Chromium(III) nitrate nonahydrate ($Cr(NO_3)_3 \cdot 9H_2O$, 99 wt.%) was purchased from Sigma-Aldrich. Copper(II) nitrate trihydrate ($Cu(NO_3)_2 \cdot 3H_2O$, 99–102 wt.%) was purchased from Alfa Aesar. Ammonia hydroxide ($NH_3 \cdot H_2O$, 25–28 wt.%), hydrofluoric acid (HF, 40 wt.%) and isopropanol (99.8 wt.%) were purchased from Aladdin. Perchloric acid solution ($HClO_4$, 70 wt.%) was purchased from Acros Organics. 2,2'-dipyridylamine (DPA, >99.0 wt.%) was purchased from TCI. Acetone (>99.5 wt.%) was purchased from Sinopharm Chemical Reagent. Formaldehyde (37–40 wt.%) was purchased from Xilong Scientific. Commercial Pt/C (20 wt.%) was purchased from Tanaka Kikinzoku. Nafion solution (D520, 5 wt.%) was purchased from Dupont. Deionized water was used in all experiments and prepared using an ultrapure purification system. All chemicals were used as received without further purification.

Synthesis of hollow mesoporous carbon sphere (HMPCS)

This synthesis was optimized from a previous report.[1] Silica@silica resorcinol-formaldehyde nanospheres (SiO_2@SiO_2-RF) were first prepared by a hard template method.[2] Briefly, 70 mL of ethanol, 10 mL of deionized water and 3.0 mL of $NH_3 \cdot H_2O$ were added into a flask and stirred for 15 min at room temperature, and then 1.75 mL of TPOS and 1.75 mL of TEOS were added into the flask. Then, a freshly prepared resorcinol solution (0.4 g of resorcinol in 2.0 mL of ethanol) and 0.56 mL of formaldehyde were added into the flask. After stirring at room temperature for 24 h, the obtained SiO_2@SiO_2-RF nanospheres were collected by centrifugation, washed with ethanol several times, and then dried at 60 °C overnight. Subsequently, the SiO_2@SiO_2-RF was pyrolyzed at 900 °C (5 °C min^{-1}) for 5 h under N_2 atmosphere. The obtained black powder was soaked in 20 wt.% HF solution to remove SiO_2, after which the obtained HMPCS were collected by centrifugation, and washed with deionized water for several times and then dried at 60 °C overnight.

Synthesis of ternary PtCrCu catalysts

Typically, 30.0 mg of $Pt(acac)_2$, 15.3 mg of $Cr(NO_3)_3 \cdot 9H_2O$, 9.2 mg of $Cu(NO_3)_2 \cdot 3H_2O$ and 45.0 mg of HMPCS were added to 15 mL acetone. After the mixture stirring at 500 rpm for 5 h, 26.1 mg of DPA was added for another 24 h. Subsequently, the mixture was dried by rotary evaporation. The obtained powder was then pyrolyzed at 750 °C (5 °C min^{-1}) for 2 h under 10 vol.% H_2/Ar atmosphere to obtain PtCrCu. The same molar amount of Pt and transition metals were used to prepare PtCr, PtCu.

Characterization

TEM images were collected on a Hitachi HT-7700 instrument. The XRD patterns were obtained on a Bruker D8 Advance X-ray diffractometer with a Cu Kα radiation source. The AC-HAADF-STEM images and corresponding EDX elemental mappings were obtained on a JEM-ARM 300F GRAND ARM operated at 300 kV equipped with Cs correctors. XPS data were collected on a Thermo Scientific K-Alpha, using a monochromatic Al Kα radiation (1,486.6 eV). The XPS spectrum was calibrated against the C 1s peak at 284.8 eV. Metal contents in the catalyst were measured by ICP-MS PerkinElmer NexION 300X instrument.

CO-stripping measurements

CO-stripping tests were conducted by first bubbling CO into a 0.1 M $HClO_4$ electrolyte and holding potential at 0.1 V for 10 min, followed by bubbling Ar into the electrolyte for 30 min. Then, a cyclic voltammetry curve was collected by scanning from 0.05 V to 1.05 V (vs. RHE) at a scanning rate of 20 mV s^{-1}.

RDE measurements

RDE measurements were performed on a CHI Electrochemical Station (Model 760E and 7001E) equipped with a three-electrode electrochemical cell at room temperature. A saturated calomel electrode (SCE) was used as a reference electrode and a Pt foil as a counter electrode. The reference electrode potentials in this work were calibrated to the RHE potentials under H_2-saturated 0.1 M $HClO_4$ solution. The catalysts were dispersed into a mixture of ultrapure water, isopropanol and 5 wt.% Nafion solution (volume ratio of ultrapure water, isopropanol and Nafion solution was 495:495:10) by ultrasonication to form a uniform ink with a concentration of 4 mg mL^{-1}. Then 5 μL of catalyst ink was dropped onto the working electrode (a glassy carbon disk with

a diameter of 5.0 mm) and the resulting working electrodes dried in air. After drying, the catalysts were electrochemically activated in N_2-saturated 0.1 M $HClO_4$ solution at a scan rate of 500 mV s^{-1} to achieve a stable state. Subsequently, the ORR polarization curves were obtained from 0.05 to 1.1 V *vs.* RHE in O_2-saturated 0.1 M $HClO_4$ solution with a scan rate of 10 mV s^{-1} and a rotating speed of 1600 rpm.

The mass related kinetic current density (J_k) of catalyst at 0.9 V *vs.* RHE was calculated according to the equation:

$$J_k = \frac{J_L \times J}{J_L - J} \tag{1}$$

where J and J_L represent the current density at 0.9 V *vs*. RHE and the diffusion limited current density respectively. The solution resistance was measured at open circuit voltage, and the final ORR polarization curve was obtained with 95% iR correction. The mass activity (MA) was calculated by $MA = J_k / L_{Pt}$, where L_{Pt} represents the Pt loading.

The electrochemical active surface area (ECSA) was calculated from the cyclic voltammetry (CV) curve. CV was measured in N_2-saturated 0.1 M $HClO_4$ from 0.05 to 1.1 V *vs*. RHE at 50 mV s^{-1}. The ECSA was calculated according to the equation:

$$ECSA = \frac{S_{H_{upd}} \times v}{0.21 \times L_{Pt}} \tag{2}$$

where S_{H_2}, v, and L_{Pt} represent the integrated area of the H_2 desorption peak, sweep speed, and Pt loading, respectively.

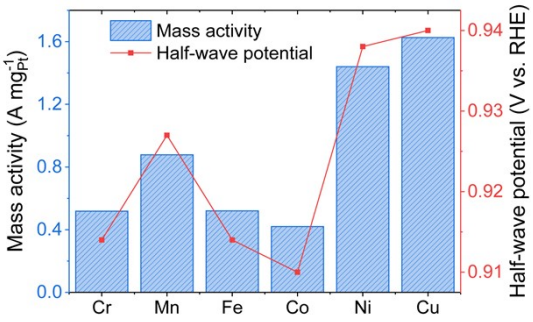

Figure S1. Comparison of oxygen reduction reaction performance with different third transition metals.

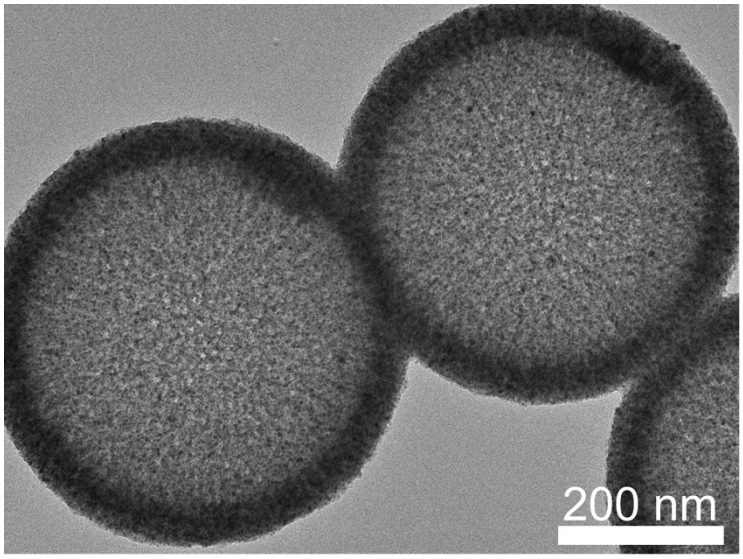

Figure S2. TEM image of PtCrCu catalysts on hollow mesoporous carbon sphere.

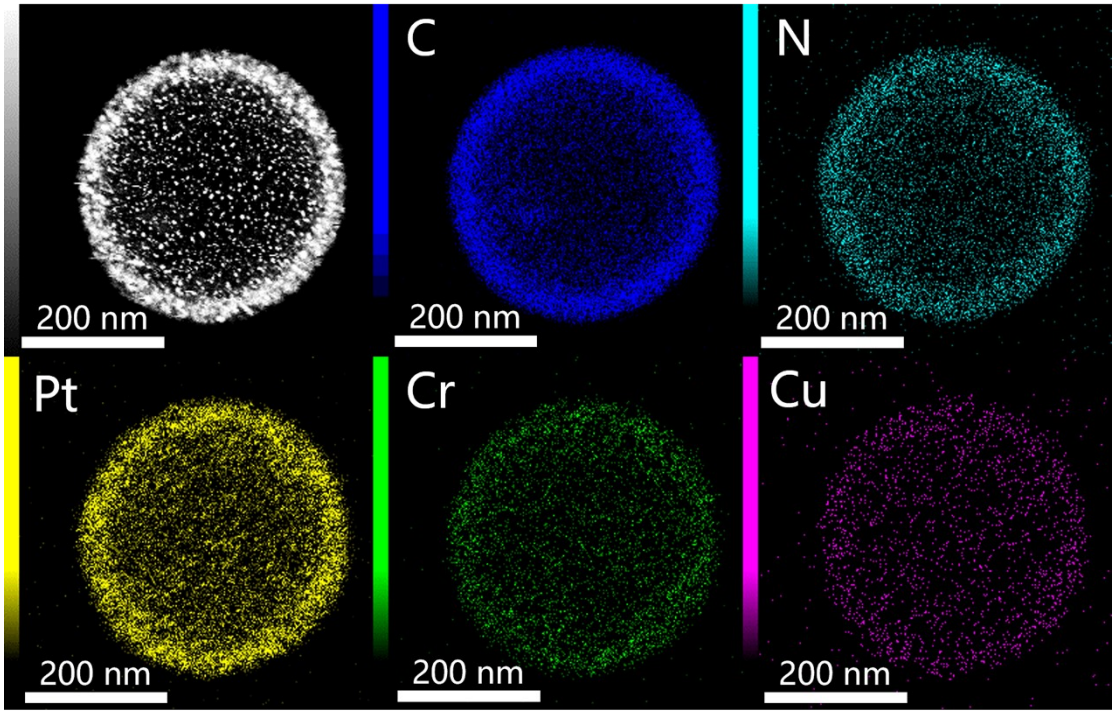

Figure S3. Elemental mapping of a single carbon sphere showing the distribution of Pt, Cr, Cu, C, and N.

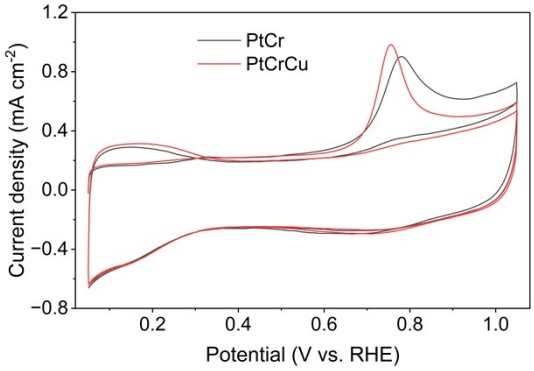

Figure S4. CO-stripping voltammograms of PtCr and PtCrCu catalysts in 0.1 M $HClO_4$, showing an apparent cathodic shift of the CO oxidation peak for PtCrCu.

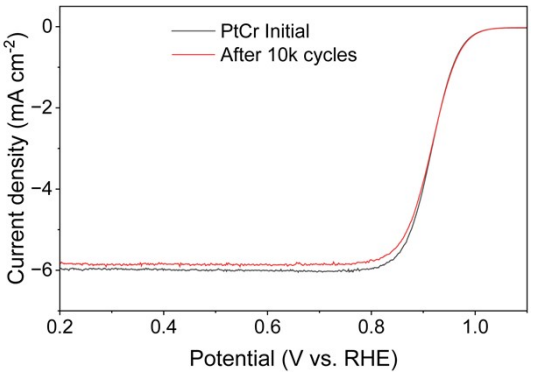

Figure S5. ORR durability of PtCr evaluated by LSV in O_2-saturated 0.1 M $HClO_4$.

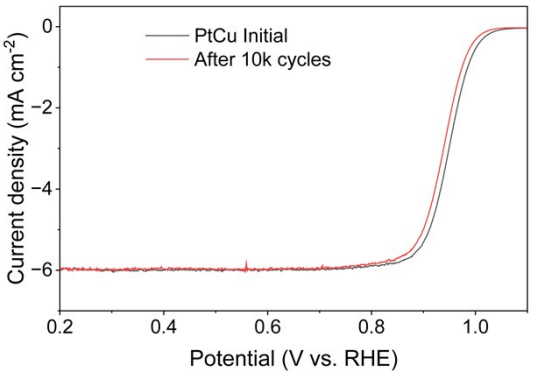

Figure S6. ORR durability of PtCu evaluated by LSV in O_2-saturated 0.1 M $HClO_4$.

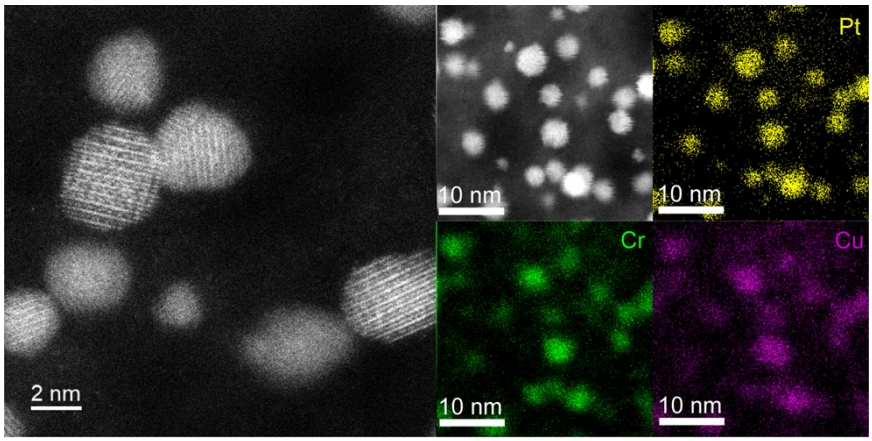

Figure S7. AC-HAADF-STEM image and EDS mapping of PtCrCu after ADT.

Table S1 Performance comparisons of PtCrCu catalyst in this work and several representative results. NA, not available.

Catalysts	MA @0.9V vs. RHE	MA Retention (%)	Ref.
PtCrCu	1.63	98	This work
Rh-Pt NWs	1.41	91.8	[3]
Pt−Fe@NC/SWCNHs	1.53	72.5	[4]
$PtNi_3$@OMC-A	2.11	79.2	[5]
Pt56Mn44	0.53	96	[6]
Pd-Pt icosahedra	1.23	88.6	[7]
PNS-Pt/C	1	86	[8]
Pt_3Fe zNWs/C	2.11	85.3	[9]
PtNiRh NWs/C	2.88	87.2	[10]
PtCoNiMo	0.45	78	[11]

Table S2. ICP-OES results of PtCrCu catalyst.

Sample	Pt (at.%)	Cr (at.%)	Cu (at.%)
PtCrCu	49.27	24.87	25.88

References

1 P. Qin, D. Liu, C. Li, G. Peng, G. I. N. Waterhouse, Y. Han, J. Shui, M. Luo, L. Shang, S. Guo and T. Zhang, *J. Am. Chem. Soc.*, 2026, **148**, 9563–9571.

2 X. Wan, H. B. Wu, B. Y. Guan, D. Luan and X. W. (David) Lou, *Adv. Mater.*, 2020, **32**, 1901349.

3 H. Huang, K. Li, Z. Chen, L. Luo, Y. Gu, D. Zhang, C. Ma, R. Si, J. Yang, Z. Peng and J. Zeng, *J. Am. Chem. Soc.*, 2017, **139**, 8152–8159.

4 S. He, Y. Liu, H. Zhan and L. Guan, *ACS Catal.*, 2021, **11**, 9355–9365.

5 K. Wang, Y. Wang, S. Geng, Y. Wang and S. Song, *Adv. Funct. Mater.*, 2022, **32**, 2113399.

6 Y. Nie, Y. Sun, B. Song, Q. Meyer, S. Liu, H. Guo, L. Tao, F. Lin, M. Luo, Q. Zhang, L. Gu, L. Yang, C. Zhao and S. Guo, *Angew. Chem., Int. Ed.*, 2024, **136**, e202317987.

7 M. Liu, Z. Lyu, Y. Zhang, R. Chen, M. Xie and Y. Xia, *Nano Lett.*, 2021, **21**, 2248–2254.

8 B.-A. Lu, L.-F. Shen, J. Liu, Q. Zhang, L.-Y. Wan, D. J. Morris, R.-X. Wang, Z.-Y. Zhou, G. Li, T. Sheng, L. Gu, P. Zhang, N. Tian and S.-G. Sun, *ACS Catal.*, 2021, **11**, 355–363.

9 M. Luo, Y. Sun, X. Zhang, Y. Qin, M. Li, Y. Li, C. Li, Y. Yang, L. Wang, P. Gao, G. Lu and S. Guo, *Adv. Mater.*, 2018, **30**, 1705515.

10 K. Li, X. Li, H. Huang, L. Luo, X. Li, X. Yan, C. Ma, R. Si, J. Yang

and J. Zeng, *J. Am. Chem. Soc.*, 2018, **140**, 16159–16167.

11 L. Huang, M. Wei, N. Hu, P. Tsiakaras and P. Kang Shen, *Appl. Catal., B*, 2019, **258**, 117974.